Chalcogenide Letters Vol. 18, No. 4, April 2021, p. 191 - 200

Effect of substrate temperature on the structural, optical and electrical properties of Tin Oxide thin films

R. N. Jayaprakash*, R. Mariappan
Department of Physcis, Adhiyamaan College of Engineering (Autonomous), Hosur-635 109, Tamilnadu, India

Interesting semiconductor materials of SnO_2 thin films were deposited on the glass substrates heated at different temperatures from 300 to 450°C. The structural, surface morphological, composition, optical and electrical properties of SnO_2 thin films were investigated. X-ray diffraction showed that the obtained films were polycrystalline nature with cubic structure and were preferential oriented along the (100) direction. The surface morphology of the films was found to increase in size when the temperature is increased from 300 to 450°C. The composition of these films was also confirmed by energy dispersive analysis by X-ray. Optical properties of the films showed high transmittance maximum at 450 nm for each spectrum is observed as about 82, 86, 87 and 89% respectively. Optical band gap energy was found to be increases from 3.52 to 3.65 nm for the SnO_2 films heated from 300 to 450°C. On the other hand, PL spectra of all films with a very sharp peak below 462 nm due to the presence of interstitial oxygen vacancies. Thus, the deposited material shows a potential application in SnO_2 thin films and might be useful for gas sensor applications.

(Received February 10, 2021; Accepted April 15, 2021)

Keywords: Nebulizer spray, SnO_2 thin films, Optical properties, Electrical properties

1. Introduction

SnO_2 is an interesting semiconductor because its sensing properties are sensible to modifications in the lattice parameters. The lattice parameters values can change due to incorporation of chemical elements different to tin oxide or by excess or deficiency of the same and it normally occurs during the synthesis process [1]. The changes in lattice parameters normally modify the surface defect states of the semiconductor and they produce variations in optoelectronic properties of the semiconductor, depending of deep or shallow nature of intrinsic defects [2]. These defects determine the SnO_2 performance in experimental applications, controlling the lifetime of charge carriers [3]. The band gap variation and photo-luminescent properties of SnO_2 have been associated to oxygen interstitials [4].

One of the main environmental applications of nanotechnology is in the water sector. heterogeneous photocatalysts, one of the advanced oxidation process(AOPS), is a cost-effective treatment methods for the removal of toxic pollutants from industrial waste water sowing to its ability to convert these into safer and products such as CO_2 and H_2O and mineral acids [5]. Several conventional methods have been used for synthesis of tin oxide nanoparticles like chemical vapour synthesis [6], laser ablation [7]), solvothermal [8], thermal decomposition [9], and sol-gel method [10]. Here we present a simple Co-precipitation method to synthesize uniform, spherically shaped and pure SnO_2 nanoparticles using tin oxide as a metal precursor and ammonium hydroxide as a precipitating agent. In the present study was report the synthesis of SnO_2 nanoparticles using Co precipitation method and the characterization of SnO_2 nanoparticles using X-Ray diffraction (XRD), transmission electron microscopy (TEM), selected area electron diffraction (SAED), scanning electron microscopy (SEM), fourier transform infrared spectroscopy (FTIR) energy dispersive spectrum (EDS) are discussed [11].

Nowadays there is a great interest for controlling the structural characteristics in different morphologies like wires, rods, nanotubes, nanorods, nanoflakes and sunflowers from the synthesis

* Corresponding author: hodprakashace@gmail.com

https://doi.org/10.15251/CL.2021.184.191

of SnO_2 [12-20]. The common methods to prepare SnO_2 are precipitation, hydrolysis, pyrolysis, solvo-thermal, sol-gel and more recently, the green synthesis [21-25]. Methanol, ethanol, acetone, ethylene-glycol, and plant extracts in the case of green synthesis, are the most used polar solvents for the synthesis of SnO_2 [26-29]. It is worth mentioning that polar solvents play an important role not only in the synthesis methods but the crystalline stability and optoelectronic characteristics of SnO_2. It was possible to obtain cubic structure SnO_2 with adequate characteristics for gas sensor applications.

2. Experimental details

Analytical grade tin (IV) chloride and sodium hydroxide pellet were used for the film preparation. Pure SnO_2 films deposited at various substrate temperature from 300 ^oC to 450 ^oC with film thickness as 222 nm, 227 nm, 232 nm and 239 nm through nebulizer spray pyrolysis (NSP) technique.Schematic diagram of the NSP setup described elsewhere. The spray solution was prepared by dissolving 0.1 M tin (IV) chloride dissolved in 50 ml of de-ionized water and the solution was stirred for 10 minutes using magnetic stirrer. For increasing the solubility of the solute few drops of concentrated hydrochloric acid was added to the solution. The mixed solutions were stirred well and heated for three hours at 60°C. This solution was sprayed onto glass substrates heated at temperatures 300, 350,400, and 450°C in air. The optimized preparative parameters for SnO_2 thin films are listed in Table1.

Table 1.Optimized preparative parameters of SnO_2 films.

Deposition rate	0.5 ml/minutes
Substrate temperature (˚C)	300˚C to 450 ^oC
pH of the solution	5
Deposition time (minutes)	10 minutes
Nozzle to substrate distance	10 cm
Carrier gas pressure	30 Pa

X-ray diffraction data of the nebulizer sprayed undoped SnO_2 films were recorded with the help of X-ray diffractometer (XPERT PRO PAN, Netherlands) with CuKα radiation (λ =0.1540 nm). Thickness of the deposited films was estimated using a stylus profilometer (Miltutoyo SJ-301). The surface morphological studies were performed using a high resolution scanning electron microscope (JEOL JSM 840). The composition of the SnO_2 thin films was analyzed by an EDAX microscopic analytic unit connected to a scanning electron microscope. Optical absorption spectrum was recorded using a UV-VIS-NIR spectrophotometer (Lambda 35). Photoluminescence spectrograph recorded on the "FP-6500 spectroflurometer". Impedance measurements were carried out using the Frequency Response, Solartron, Model 1360 coupled with the Solartron Dielectric Interface, 1296.

3. Results and discussion

3.1. X-ray diffraction analysis

Study of varying the temperature of deposition is the main step, which will increase the crystallinity, stochiometry and other structural related defects of oxide films. Fig. 1 shows the XRD of SnO_2 films deposited at different substrate temperatures of 300, 350, 400 and 450 ºC in air atmosphere.Even at a lower temperature of 300 ºC, the peaks corresponding to SnO_2 phase started appearing. From the figure, it is observed that the films are polycrystalline with preferred orientation along (200). Other XRD peaks pertain to (110), (101), (211), (310) and (301) directions

are also present. All the diffraction peaks seen in the Fig. 1 confirm the tetragonal rutile structure of the nebulizer spray coated SnO_2 films. Temperature increases the intensity of the preferred orientation of (200) indicating an increased crystallinity with temperature. The intensity of the (110), (101), (211), (310) and (301) peaks also increase with temperature. However no other phases like SnO and SnO_x usually found at elevated temperatures, have been observed in the present nebulizer spray coated SnO_2 films prepared by spraying in the temperature range 300 –450 ^oC.

It is an interesting result that the developed XRD peaks are found in the films heated even at a relatively temperature of 450 ^oC in the present study. RakhiKhandelwaln et al., [30] have reported sharp peaks for their SnO_2 films prepared by spray pyrolysis technique at deposition temperatures ranging from 150 to 400 ^oC. Similarly using the spray technique, Saji Chacko et al [31] have obtained good polycrystalline and oriented SnO_2 films at temperatures range 400-500 ^oC. Present results show that the nebulizer coating technique is capabable of providing polycrystalline SnO_2 films with temperature 450 ^oC.

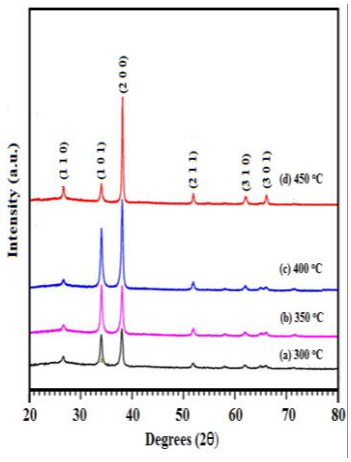

Fig. 1.XRD pattern of SnO_2thin films.

The hkl and d values for the SnO_2 films deposited at different temperatures are agreeing well with the values found in JCPDS card. The calculated values of lattice parameters, a = 4.786 Å and c = 3.171 Åare in very good agreement with the reported values of a = 4.772 Å and c = 3.170 Årespectively. The crystallite size (D) was calculated from the full width at half maximum (FWHM) β of the prominent XRD peaks using the Scherrer-Bragg relation.

The variation of micro structural parameters like grain size, dislocation density, strain and number of crystlalites with deposition temperature is listed in Table 2. It shows that the grain size reaches a maximum 66 nm (200 plane) at 450^{o}C. The crystallite size varies in the range from 33 nm to 66 nm as the temperature of SnO_2 film deposition increases from 300 to 450^{o}C. It is observed that the Table 2, the dislocation density and micro strain are found decreasing upto 450^{o}C.

Table 2. To calculated the structural parameters of SnO_2 thin films.

Temperature (^oC)	(hkl) Crystal System	(Debye-Scherrer) Crystallite Size (nm)	Dislocation Density, δ (10^{14}lin/m^2)	Micro Strain,ε (10^4 $lin^{-2}m^{-4}$)
300 ^{o}C	110	28.836	12.02	11.70
	101	33.179	09.08	09.42
	200	33.355	08.98	08.89
	211	21.007	22.65	09.26
	310	08.856	126.6	19.92
350 ^{o}C	110	46.120	04.70	07.32
	101	46.439	04.64	06.72
	200	38.895	06.61	07.63
	211	31.497	10.07	06.18
	310	32.503	09.46	05.45
400 ^{o}C	110	28.837	12.02	11.69
	101	58.048	02.96	05.37
	200	59.185	05.73	05.16
	211	41.986	05.67	04.64
	310	32.503	09.46	05.45
450 ^{o}C	110	28.838	12.02	11.68
	101	38.705	06.67	08.05
	200	66.682	02.24	04.45
	211	25.201	15.74	07.73
	310	21.668	21.29	08.17

3.2. Surface morphological analysis

The surface morphology of SnO_2 films deposited at 300, 350, 400 and 450 ^{o}C are shown in Fig. 2a-c. Is is observed that the Fig. 2a, the uniform surface and tiny grain with average grain size ~250 nm at 300^{o}C. The grain growth and smoothness of the surface improved at the temperature 350 and 450^{o}C. Grains are found to grow with increased temperature. Uniform surface morphology with larger grains is observed on the surface of SnO_2 films at 450^{o}C. No cracks or pin holes are seen and the scanned surfaces are uniformly covered with inter connected grains showing very limited grain boundary area.

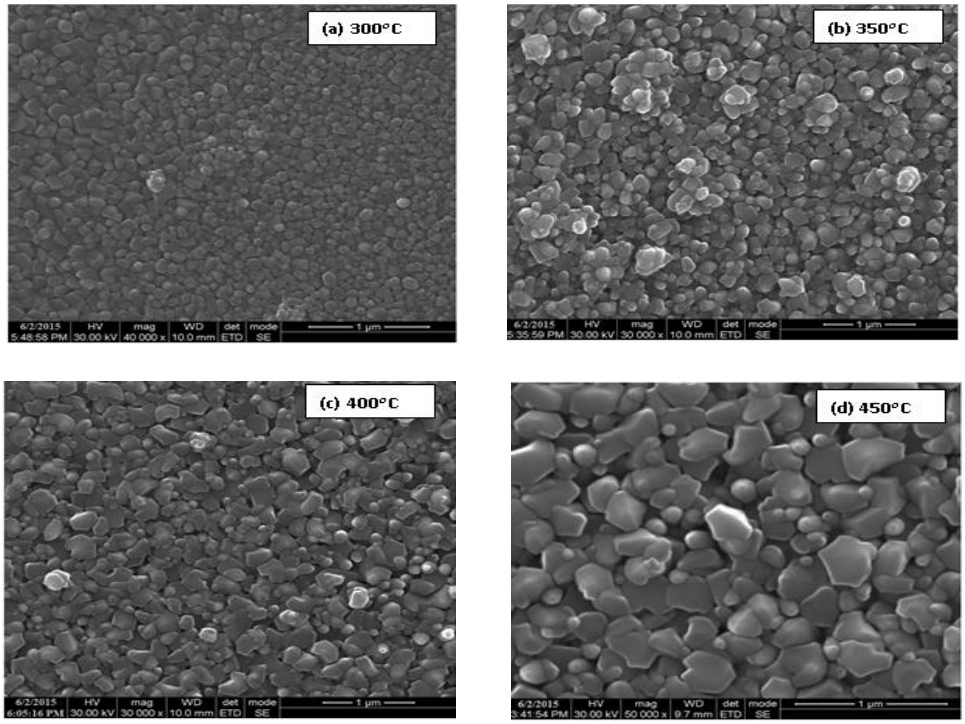

Fig. 2. HRSEM images of SnO_2 thin films.

At 450^{o}C, the films show slightly less uniform surface morphology with patches of materials as seen in Fig. Fig.2d. These morphological changes with deposition temperature show that grains are found to increase in size when the temperature is increased from 300 to 450^{o}C. The formation of larger grains may be attributed to the aggregation or fusion of small particles at higher temperatures. From these morphological results it is observed that uniform SnO_2 films can be prepared by keeping the substrate temperature from 300 to 400^{o}C in the present study of nebulizer spray pyrolysis technique.

3.3. Energy dispersive analysis by X-ray spectroscopy (EDX)

The stoichiometry analysis of the elements present in the SnO_2 thin film was carried out by EDX results. Fig. 3 shows the EDX pattern of the SnO_2 film deposited under the optimized conditions deposited temperature from 300 to 450^{o}C. From the EDX spectrum it is observed that the prepared SnO_2 has nearly the stoichiometric ratio of Sn and O but with oxygen deficiency. The ratio of Sn:O is found to be 52.98 : 47.02. This is clear evidence that this oxygen deficiency gives lower resistivity to SnO_2 films heated at 450^{o}C in the present study.

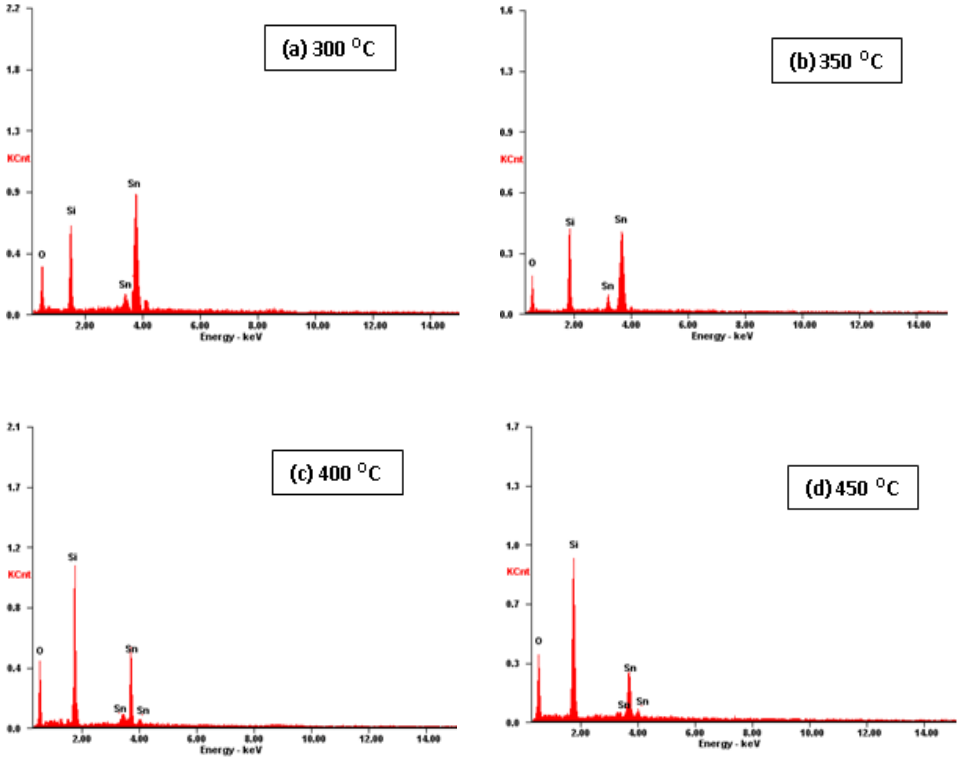

Fig. 3. EDX patterns of SnO_2 thin films.

3.4.Optical properties

3.4.1. UV-Vis analysis

Fig. 4 shows the transmission spectra in the wavelength region of 200-2500 nm for the SnO_2 films deposited at different heating temperatures 300, 350, 400 and 450 ºC. The transmittance maximum at 450 nm for each spectrum is observed as about 82, 86, 87 and 89% respectively.

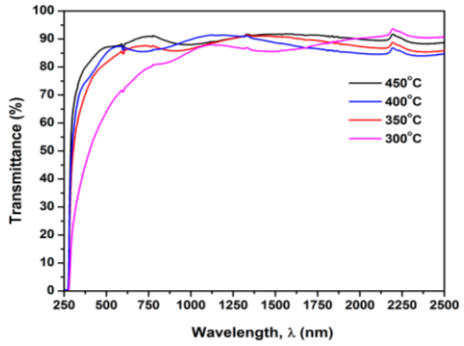

Fig. 4.Transmittance spectrum of SnO_2 thin films.

The average percentage transmission for all the SnO_2 films is in the recorded wavelength region of 200-2500 nm. It is observed that as the heating temperature increases, the percentage of transmission increases. Maximum percentage transmission is recorded for the SnO_2 film deposited at a temperature of 450ºC are shown in Fig. 4.

It is reported that SnO_2 semiconductor oxide film is a degenerate semiconductor material with band gap values (E_g) varying in the range of 3.45 to 4.58eV [32, 33]. These wide scatter in the band gap of SnO_2 may be due to the varied extent of oxygen non-stoichiometry of the deposited films in different techniques. The correlation between the band gap and the carrier

concentration has been explained [33]. It has been related that the band gap energy increases linearly with the increase of carrier concentration to the power of 2/3.

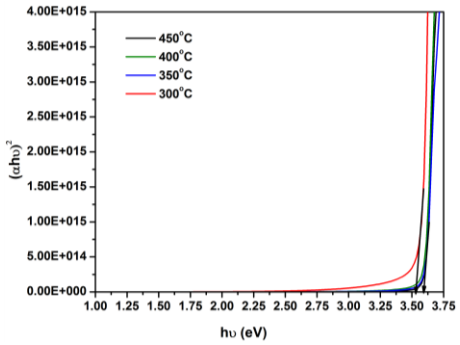

Fig. 5. Plots of $(\alpha hv)^2$ versus (hv) for the SnO_2 films.

The variation of $(\alpha h\nu)^2$ versus (hν) for the SnO_2 films deposited at different temperatures is shown in Fig. 5. The straight line portion indicates that the optical transition is direct in nature. The direct gap value has been determined by extrapolating the vertical straight line portion of the plot to the energy axis. The intercept on energy axis gives the values of band gap energy from 3.52 to 3.65 nm for the SnO_2 films heated from 300 to 450^{o}C. These values are higher than the value of Eg = 3.57eV reported for single crystal SnO_2 [34].

Semiconductor films often show a band gap widening and the absorption edge moves towards the shorter wavelength side (blue shift) than that of the bulk semiconductor material. However, when SnO_2 is prepared with oxygen deficiency (SnO_{2-x}) and when the carrier concentration is of the order of 10^{20} cm^{-3}, a substantial band gap widening is also reported [35]. Similar results have been observed for spray deposited SnO_2:F and SnO_2:Sb films [36]. The onset of light absorption is shifted towards lower wavelength side in semiconductor oxide films, especially for the highly non-stoichiometric oxide films with large carrier concentrations. These results show that SnO_2 film deposited at 450^{o}C with sprayed coating has good optical transmission property and higher band gap value.

3.4.2.Photoluminescence studies

The room temperature photoluminescence (PL) spectra of SnO_2 films with various substrate temperatures from 300 ^{o}C to 450 ^{o}C are shown in Fig. 6. PL emission spectra of the all films were recorded in the wavelength range of 350 nm to 500 nm at an excitation wavelength 325 nm.

The PL property of the films has a close relation with the film crystallinity because the density defect in film reduces with an improvement of the crystallinity. It is observed from Fig. 6, that there are two emission bands in the spectra: a sharp ultra-violet (UV) near-band emission peak centered around 392 nm (3.11 eV) and a sharp visible deep-level green emission centered around 462 nm (2.65 eV) for the ZnO films. This ultra-violet peaks can be attributed to the oxygen vacancies in ZnO. From Fig.6 show the PL spectra of all films with a very sharp peak below 462 nm due to the presence of interstitial oxygen vacancies. In conclusion that the origin of the blue-green emission is due to transition from conduction band to the acceptor level corresponding to the antisite of oxygen [36, 37].

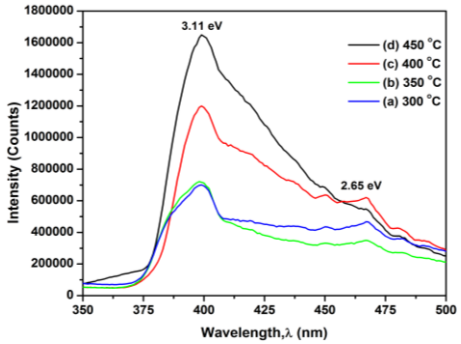

Fig. 6. PL studies of SnO_2 thin films.

3.5. Electrical properties

3.5.1. Impedance analysis

Fig. 7 shows the real ($Z^{/}$) and imaginary ($Z^{//}$) (Nyquist plots) parts of the in the complex impedance spectra and the corresponding equivalent circuits of SnO_2 thin films studied at temperatures from 300 to 450^{o}C.At high frequency, the data show a semicircle indicating that the relaxation time of the bulk and the grain boundaries are close to each other. In the mid frequency range, a linear progress in the diffusion characteristics of SnO_2 is observed during insertion-desertion process. In the lowest frequency area, capacitive behavior is observed showing the characteristic response of a finite blocked diffusion. Centre of the semicircle is localized below real axis is ascribed to constant phase element. Intersect on the real axis of the semicircle at low frequencies is ascribed to the total resistance. Conversely, the impedance response of grain dominates at high frequencies and resistances of grain (R_g) is deduced from the left intersect of the semicircle to real axis.

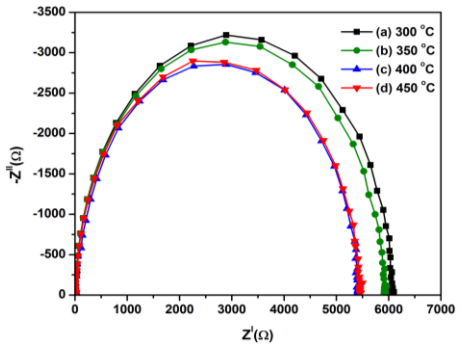

Fig. 7. Impedance spectroscopy studies of SnO_2 thin films.

The intercept of semicircle to real axis ($Z^{/}$) at low frequency depicts the sum of resistance of grains and grain boundaries while an intercept at high frequency depicts the resistance of grain only. Grain boundary resistance decreases with temperature is due to the grain boundary effect which has assisted the lowering of the motion of charge carriers.

4. Conclusions

The nebulizer spray pyrolysis coating has been used to prepare highly transparent as well as conducting SnO_2 films. X-ray diffraction confirm the tetragonal structure with preferred orientation along (200) plane. Crystallite size is found to be increased from 33 nm to 66 nm with various temperatures from 300 to 450 ^{o}C. The scanning electron microscopy studies reveal that the tin oxide (SnO_2) film demonstrates many spherical like grains. The average grain sizes of the

grains are in the range of 250 to 500 nm at 450 ^{o}C. The presence of elemental constituents was confirmed from energy dispersive X-ray analysis.The maximum optical transmittance 89% was obtained for SnO_2 film deposited at substrate temperature (450 ^{o}C). From the optical studies it is observed that the band gap energy increases from 3.52 to 3.65 eV with increase of temperature.The photoluminescence spectra observed that all the films were able to generate violet and green emission in the visible region. The intensities of defects emission decrease with the increase of substrate temperature leading to the green shift emission in the PL spectra of SnO_2 films. The impedance spectroscopy measurements performed on the films show a very strong resistance decreases when the temperature increases from 350 to 450^{o}C.The present study clearly shows that device quality and uniform grained SnO_2 films can be prepared with a low resistance of about 5500 Ω with small grains. A high band gap of 3.58 eV can be prepared by the nebulizer spray technique by depositing at a temperature of 450 ^{o}C. The investigation results of the SnO_2 films prepared by NSP technique ensure the stability of the films and their employability in optoelectronics device applications.

Acknowledgements

Authors thankful to the Adhiyamaan College of Engineering (Autonomous), Hosur and Indian Institute of Science, Bangalore.

References

[1] R.C.Garvie, R.H. Hannink, R.T. Pascoe, Nature **258**, 703 (1975).
[2] J.F. Haw, J. Zhang, K. Shimizu, T.N. Venkatraman, D.P. luigi, W. Song, D.H. Barich, J.B. Nicholas, J. Am. Chem. Soc. **122**, 12561 (2000).
[3] SH.M. Abed, S.N. Turki AL-Rashid, Chalcogenide Letters **15**, 237 (2012)
[4] V. Janakiraman, V. Tamilnayagam, R.S. Sundararajan, S. Sivabalan, B. Sathyaseelan, Chalcogenide Letters **17**, 405 (2020)
[5] N. Mansour, K. Mansour, E.W.V. Stryland, M.J. Soileau, J. Appl. Phys. **67**, 1475 (1990).
[6] J. Li, G.W. Hastinhs, Oxide Bioceramics: Inert Ceramic Materials in Medicine and Dentistry, Chapman & Hall, London, New York, 340 (1998).
[7] M. Tahmasebpour, A.A. Babaluo, M.K. RazaviAghjeh, Journal of the European Ceramic Society **28**, 773 (2008).
[8] L. Liang, Y. Xu, D. Wu, Y. Sun, Materials Chemistry and Physics **114**,252 (2009).
[9] L. Gahramanli, M. Muradov, O. Balayeva, G. Eyvazova, Chalcogenide Letters **16**, 587 (2019)
[10] J.J. Yu, J.Y. zhang, I.W. Boyd, Applied Surface Science **168**, 190 (2002).
[11] K. Prasad, D.V. Pinjari, A.B. Pandit, S.T. Mhaske, Ultrasonic Sonochemistry**18**, 1128 (2011).
[12] Iqbal Ahmed Siddiquey, Takeshi Furusawa, Masahide Sato, Newaz Mohammed Bahadur, Md. Nizam Uddin, Noboru Suzuki, Ceramics International **37**, 1755 (2011).
[13] K. Aslan, C. D. Geddes, Plasmonics**3**, 89 (2008).
[14] E.B. Celer, M. Jaroniec, J. Am. Chem. Soc. **128**(44), 14408 (2006).
[15] M. Tsuji, M. Hashimoto, Y. Nishizawa, M. Kubokawa, T. Tsuji, Chem. Eur. J. **11**(2), 440 (2005).
[16] Y.J. Zhu, W.W. Wang, R.J. Qi, X.L. Hu,Angew.Chem. Int. Ed. **43**(11), 1410 (2004).
[17] M.F. AI-Kuhaili, S.M.A. Durrani, Journal of Alloys and Compounds **509**, 9536 (2011).
[18] K. P. S. S. Hembram, G. M. Rao, Journal of Nanoscience and Nanotechnology **8**, 4159 (2008).
[19] R. Dwivedi, A. Maurya, A. Verma, R. Prasad, K. S. Bartwal, Journal of Alloys and Compounds**509**, 6848 (2011).
[20] J. Liang, Z. Deng, X. Jiang, F. Li, Y. Li, Inorganic Chemistry **41**, 3602 (2002).
[21] A. K. Singh, U. T. Nakate, Journal of Nanoparticles, 7 (2013).
[22] S. Shukla, S. Seal, R. Vanfleet, Journal of Sol-Gel Science and Technology**27**,119(2003).

[23] B. Tyagi, K. Sidhpuria, B. Shaik, R. V. Jasra, Industrial and Engineering Chemistry Research **45**, 8643 (2006).
[24] A. K. Singh, Advanced Powder Technology **21**, 609 (2010).
[25] N. ClamentSagayaSelvam, A. Manikandan, L. John Kennedy, J. Judith Vijaya, Journal of Colloid and Interface Science **389**, 91 (2013).
[26] L. A. Perez-Maqueda, E. Matijevic, Journal of Materials Research **12**, 3286 (1997).
[27] S. Chen, Y. Yin, D. Wang, Y. Liu, X. Wang, Journal of Crystal Growth **282**, 498 (2005).
[28] Kayleen Campbell, Duncan Q.M. Craig, Tony McNally, International Journal of Pharmaceutics **363**, 126 (2008).
[29] F. Kazemi, A. Saberi, S. Malek-Ahmadi, S. Sohrabi, H. R. Rezaie, M. Tahriri, Ceramics-Silikaty**55**, 26 (2011).
[30] RakhiKhandelwal, Amit Pratap Singh, Avinashi Kapoor, SorinGrigorescu, Paola Miglietta, NadyaEvgenievaStankova, AlessioPerrone, Optics & Laser Technology **41**, 89 (2009).
[31] Saji Chacko, NinanSajeeth Philip, K.G. Gopchandran, Peter Koshy, V.K. Vaidyan, Applied Surface Science **254**, 2179 (2008).
[32] J.J.PH. Elich, E.C. Boslooper, H.Haitjerma, Thin Solid Films **177**,17 (1989).
[33] B. Stjerna, E. Olsson, C.G. Granqvist, J. Appl. Phys. **76**,3797 (1994).
[34] L. Abello, B. Bochu, A.Gaskov, S. Koudryavtseva, G. Lucazeau, M. Roumyantesva, J. Solid State Chem. **135**,78 (1998).
[35] E. Shanthi, A. Banerjee, K.L. Chopra, Thin Solid Films **88**,93 (1982).
[36] E. Czapla, E. Kusior, M. Bucko, Thin Solid Films **182**,15 (1989).
[37] S. Singh, N. Jahan, A. Khanna, G. Singh, N.K. Verma, Chalcogenide Letters **9**, 73 (2012)